Building form influence on energy flexibility in different utility pricing schemes

Samson Yip, Andreas Athienitis, Bruno Lee
Centre for Zero Energy Building Studies, Concordia University, 1455 de Maisonneuve West, EV 6.139, Montreal, QC, H3G 1M8, Canada

Abstract

As more PV-clad buildings are connected to the grid, the mismatch in energy generation and demand leads to greater network stress. Using energy flexibility measures on the building side is a possible solution to this problem.

For buildings with building-integrated PV and thermal (BIPV/T) systems, the PV/T form follows the building form. Building form choices will have an influence on energy performance and energy flexibility. To quantify this, a set of BIPV/T-clad building forms with plan shape and azimuth variations was analyzed with two flexibility strategies under two utility pricing schemes. The target was peak demand reduction during winter peak periods. The configurations were compared using peak power reduction, the building energy flexibility index (BEFI), and energy cost savings.

Results showed reductions of up to 32% in peak power and 25% in energy costs. Most scenarios of azimuth/flexibility strategy under the different metrics led to a Pareto front of favourable plan shapes.

Introduction

With growing numbers of PV-equipped buildings such as net-zero energy buildings (NZEBs) being constructed and connected to the grid, the mismatch in local energy generation and demand leads to greater network stress. However, these same buildings can be part of a solution to alleviate that stress through demand-side energy flexibility strategies.

Energy flexibility is generally defined as "the ability [of a building] to manage its demand and generation according to local climate conditions, user needs, and energy network requirements," (Jensen, Marszal-Pomianowska et al. 2017). Some flexibility resources available on the demand side that have been shown to be very effective include the building's thermal mass (Le Dréau and Heiselberg 2016, Lind, Möllerström et al. 2023), water tanks (Dumoulin, Rounis et al. 2021, Gaucher-Loksts, Athienitis et al. 2022), electrical storage (Tumminia, Guarino et al. 2020), the renewable energy system, like PV (Aelenei, Lopes et al. 2019, Dumoulin, Rounis et al. 2021, Gaucher-Loksts, Athienitis et al. 2022), HVAC systems including heat pumps (Dumoulin, Rounis et al. 2021, Gaucher-Loksts, Athienitis et al. 2022), and building controls (Zhang and Kummert 2021). A few of the common energy flexibility objectives are load shifting, energy cost reduction, and peak demand reduction (Li, Johra et al. 2023).

While there exists research on the design of building form with BIPV for energy performance, the principal objective has been on optimizing form and PV placement for minimizing annual net energy use. Examples include (Ciardiello, Rosso et al. 2020, D'Agostino, Mazzella et al. 2022, Barrutieta, Kolbasnikova et al. 2023).

For research on building form with BIPV and its relationship to energy use and the grid, the focus has been on increasing PV self-consumption to increase load matching and decrease grid interaction. Different methodologies were used to determine the distribution pattern of the required number of panels, on which building surfaces, and at which azimuth and tilt angles. The investigations have been at the building (Martín-Chivelet and Montero-Gómez 2017, Aguacil, Lufkin et al. 2019, Lovati, Salvalai et al. 2019) and urban scale (Freitas, Reinhart et al. 2018, Kurdi, Alkhatatbeh et al. 2022).

However, as discussed in (Li, Johra et al. 2023), self-consumption with respect to energy flexibility relates the building's energy use in response to the state of its own renewable energy generation as opposed to an external grid signal or event. Also, there were no changes to the building load profiles or passive design.

On the other hand, (Skandalos and Karamanis 2021) considered load-matching among the objectives in an investigation of four types of BIPV applications for façade and windows that measured the active performance of the PV *and* their effect on modulating the passive solar heat gains in the room directly behind the PV-integrated windows. But this investigation did not include any building form design.

In a design investigation of a house with solarium, combinations of PV/T, heat pump, and thermal storage were used to enable energy flexibility. The options of using semi-transparent PV windows on the solarium and

using the solarium's solar heated air to supply the air-source heat pump influenced the active design and passive design (Gaucher-Loksts, Athienitis et al. 2022). This investigation did not include any building form design.

Finally, in a study involving building form and energy flexibility, the influence of thermal mass quantity was investigated in combination with BIPV/T, building plan shape, and orientation to reduce peak demand (Yip, Athienitis et al. 2021). That study showed the effect of building form on both passive and active design contribution to energy flexibility.

To evaluate energy flexibility, there exist many KPIs or metrics in the literature. They can be categorized by direct or indirect quantification; applicable phase of design; application type or flexibility objective, data requirements, baseline requirement, target stakeholders, among others (Li, Wang et al. 2021, Li, Satchwell et al. 2022, Li and Hong 2023, Li, Johra et al. 2023).

In summary, while some studies exist showing the use of building form for introspective objectives like improving building energy load-matching, not many address how building form coupled with different flexibility strategies can respond to external grid events or needs such as peak demand reduction and how that performance is measured.

Therefore, the objective of this study was to investigate building form and orientation as influencing factors on energy flexibility when designed in conjunction with different energy flexibility control strategies and measured under different metrics. The building plan shape, orientation, and controls combinations were applied to a medium-sized commercial/institutional building archetype. Simulations were carried out for winter conditions in the Montreal climate. Peak power reduction, the building energy flexibility index (BEFI), and energy cost savings under two different energy pricing schemes – one containing a peak demand charge, the other using time-of-use rates – were used to evaluate the design configurations.

Methodology

Simulation model

An automated design framework was used to generate the simulations in this paper. Details including the building simulation model, BIPVT characteristics, building archetype geometry, and their linkages is found in (Yip, Athienitis et al. 2021, Yip, Athienitis et al. 2021).

The framework was created to support early-stage design decision-making for high-performance, NZEB-level buildings with building-integrated PV and PV/T. The model parametrized a range of variables including geometric variables related to building form and orientation.

Other variables often considered at the early design stage parameterized within the framework include: insulation levels, BIPV/T characteristics (tilt angle, electrical conversion efficiency, air channel height, and channel air speed), window to wall ratio, and window properties.

Crucially, the investigation with the framework was for early-stage design – the design phase directly preceding the design development phase when building controls are first typically considered in a design project timeline.

The selection of variables and the range of values to be tested were input in python to generate the unique design configurations which were simulated in TRNSYS18 and post-processed in python.

Building-integrated PV/T

As PV becomes more prevalent in buildings, increased architectural and engineering systems integration can be achieved by designing the PV to be an integral element of the building enclosure from the early design stage. Therefore, the renewable energy technology incorporated in the automated design framework was building-integrated PV and thermal (BIPV/T). For buildings with BIPV/T systems, the PV/T form follows the building form. Therefore early design stage decisions taken on building form will have an influence on net energy performance and energy flexibility – even before detailed controls design takes place.

Building type under consideration

The building archetype investigated was a two-storey medium-sized (3 000 m^2) commercial and institutional building. A rectangle (RE), courtyard (CO), L-, and U-shaped plans were used. The L- and U-shapes have wing variations in 15° increments creating L15 to L75 and U15 to U75 shapes as shown in Figure 1. A range of orientations (ψ) from −45° to 45° in 15° increments was used to permit enhanced passive and active solar gains.

Other common design features of the building configurations include wall insulation of 6.79 m^2K/W (R38), roof insulation of 7.92 m^2k/W (R45), window to wall ratios (WWR) of 30%, 30%, 20%, 10% for south, west, east, and north orientations, respectively, a BIPV/T system electrical conversion efficiency of 17% and a tilt angle of 35°. The climate was for Montreal, QC.

Energy flexibility strategies

Two energy flexibility strategies were created based on rule-based temperature setpoint controls. The reference and flexibility control strategies are shown in Figure 2.

Flex1: The building was preheated starting at 03:00 by stepping up the setpoint temperature without surpassing the reference setpoint temperature of 21°C. At 12:00 the temperature was increased to 23°C to increase PV self-consumption and charge the thermal mass for energy discharging during the evening peak period. The profile was identical to the reference strategy after 18:00.

Flex2: The building was preheated aggressively during the early morning hours to a peak of 23°C before stepping

down to 21°C for the morning peak period. The control profile was identical to Flex1 after 08:00.

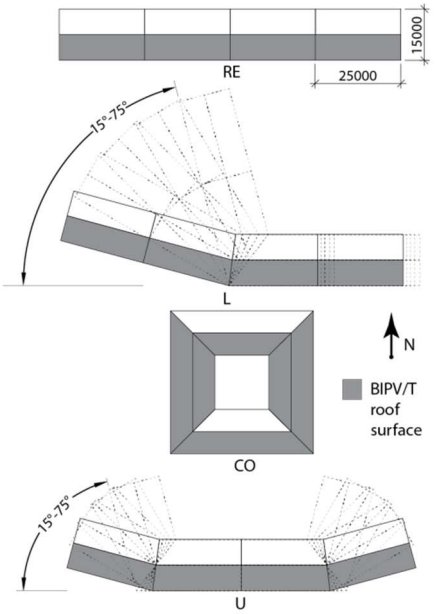

Figure 1: Plan shape families.

Rate M and TOU

For the province of Quebec, the critical period for the grid is in winter, from December to March. There are two weekday peak periods from 06:00 – 09:00 and 16:00 – 20:00 (Hydro-Québec 2024).

Rate M is the electricity billing rate for a building of the size and vocation considered in this work. Its calculation comprises a peak power (kW) and an energy (kWh) component. Subscribers are incentivized to minimize their winter peak power since 65% of this value is used to establish the minimum monthly peak power component for the next 12 months (Hydro-Québec 2023).

A three-tier time-of-use (TOU) pricing scheme was calculated using the same daily peak periods defined above with pricing based on the Ontario rate (Ontario Energy Board 2024).

Peak power reduction and BEFI

Since the energy flexibility objective was to reduce peak demand using early stage design variables, the peak power reduction, building energy flexibility index (BEFI), and energy cost savings were used as evaluation metrics.

The peak power reduction is given by

$$\Delta P_{max} = P_{ref,max} - P_{flex,max} \quad (1),$$

$$\Delta P_{max} = \left(1 - \frac{P_{flex,max}}{P_{ref,max}}\right) \cdot 100\% \quad (2),$$

where $P_{ref,max}$ is the power peak of the reference scenario and $P_{flex,max}$ is the power peak of the flexibility scenario.

The building energy flexibility index (BEFI) represents the breadth of power savings potential, that is, the average power that can be made available to the grid for the duration of a grid event such as a peak demand period (Athienitis, Dumont et al. 2020, Date, Candanedo et al. 2021, Morovat, Athienitis et al. 2021).

$$BEFI = \frac{\int_t^{t+\Delta t} P_{ref}\,dt - \int_t^{t+\Delta t} P_{flex}\,dt}{\Delta t} \quad (3),$$

$$BEFI = \frac{\int_t^{t+\Delta t} P_{ref}\,dt - \int_t^{t+\Delta t} P_{flex}\,dt}{\int_t^{t+\Delta t} P_{ref}\,dt} \cdot 100\% \quad (4),$$

where P_{ref} is the power demand of the reference scenario, P_{flex} is the power demand of the flexibility scenario, t is the start time of the demand response event, and Δt is the duration of the event.

Results and discussion

Cold sunny day performance

The graph in Figure 3 of energy performance of select plan shape, orientation, and flexibility control combinations on a cold sunny January day shows the range of possible energy performance among the tested configurations. It can be seen that the building configurations' energy profiles had the greatest impact on the grid during the morning peak demand period. This was representative of

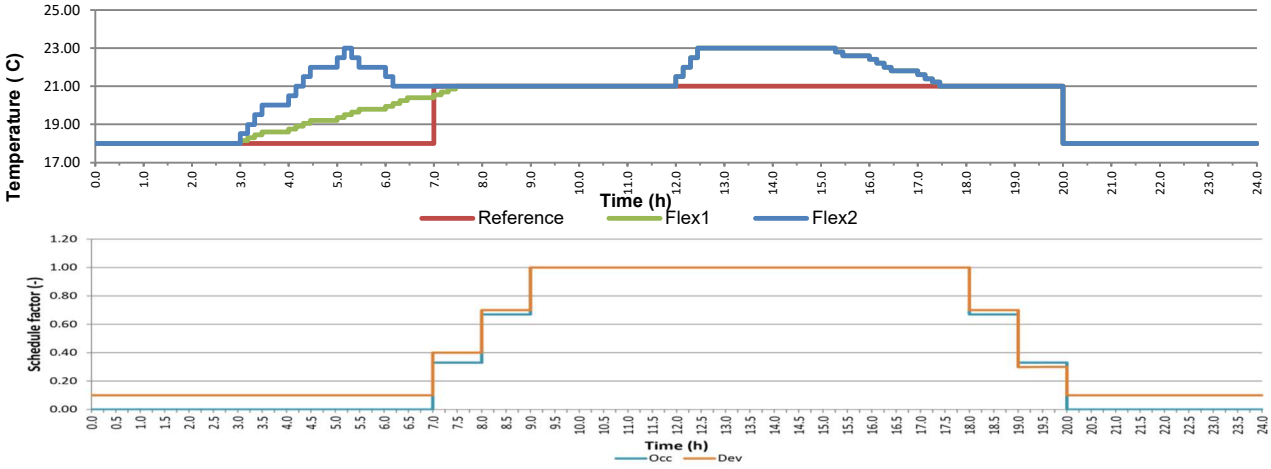

Figure 2: Top: Temperature setpoint profiles for the reference, Flex1 and Flex2 control strategies. Bottom: Occupancy (Occ) and plug load (Dev) schedules.

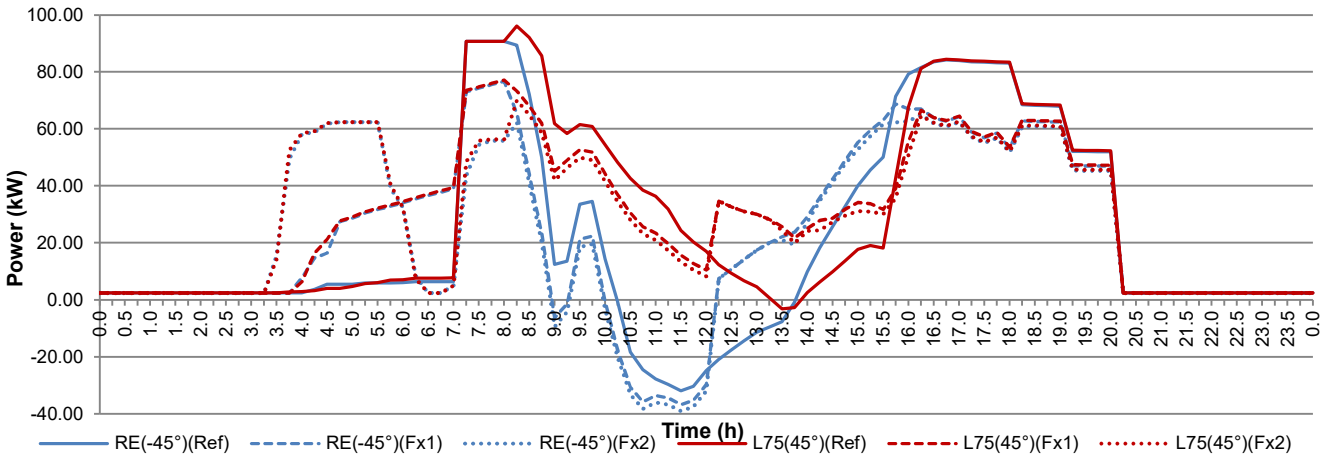

Figure 3: Power demand on a cold sunny January day for RE and L75 shapes using reference (Ref), Flex1 (Fx1), and Flex2 (Fx2) controls, at orientations of −45° and 45°.

all the tested configurations. Thus the morning peak performance was a key determinant for Rate M costs.

Examining further the morning peak period, the RE ψ=−45° configuration had a lower peak demand than the L75 ψ=45° configuration for the reference case (90.72 kW versus 96.18 kW; difference of 6%) and Flex2 (62.12 kW versus 70.03 kW; difference of 13%) control strategies. The RE ψ=−45° configuration benefitted from having a larger percentage of PV and window area biased towards the early morning sunshine hours. The solar gains helped contribute to it keeping its power demand from increasing further unlike in the L75 case. Interestingly, under the Flex1 control, the RE and L75 morning peak demand was very similar (76.66 kW versus 77.15 kW; difference of less than 1%). In this case, the continuous stepping up of the setpoint temperature levels up both configurations' power demand all the way through to the power peak at 08:00. Since both configurations reached their peak demand soon after sunrise, solar gains were not a performance differentiating factor.

In the Flex2 case, the thermal mass was highly charged by 05:30 when the power dropped off precipitously and the building came close to free-floating between 06:00 and 07:00. The power spiked up at 07:00 and 08:00 due to increases in building occupancy and reached a peak at 08:15. Unlike in the Flex1 case, the amplitude of this peak was influenced by solar gains resulting in a difference of 13% between the RE peak and L75 peak as stated above. Similarly, L75 reference power also peaked at 08:15 while the RE reference power actually decreased after 08:00 due to solar gains.

Table 1 summarizes the power values from Figure 3. As mentioned earlier in this section, solar gains were a factor at the time peak power was reached under the reference control strategy but were not under the Flex1 strategy. This explains how L75 achieved a greater peak power *reduction* of 19.0 kW (19.78%) than RE at 14.06 kW (15.50%) under the Flex1 strategy.

On the other hand, the Flex2 strategy produced the largest peak power reduction for the two plan shapes, although RE benefited the most due to increased early morning solar gains – achieving a peak power reduction of 28.60 kW (31.52%).

The BEFI results are consistent with those of peak power reduction: RE, at ψ=−45°, drew the greatest advantage due to early morning solar gains. Under Flex2, RE was able to make 22.57 kW (44.24%) of flexible power available to the grid during the morning peak demand period. Nevertheless, at ψ=45°, which benefits the least from early morning solar gains, the BEFI calculation shows L75 was still able to make 21.61 kW (35.56%) of flexible power available to the grid.

In general, increased energy performance during the morning peak period due to larger PV and window areas oriented towards morning sun was observed in all cases – under reference and flexibility control strategies.

Table 1: Peak power (P_{max}), peak power reduction (ΔP_{max}), and building energy flexibility index (BEFI).

Plan shape	ψ	P_{max}			ΔP_{max}				BEFI			
	°	Ref	Flex1	Flex2	Flex1	Flex2	Flex1	Flex2	Flex1	Flex2	Flex1	Flex2
		kW	kW	kW	kW	kW	%	%	kW	kW	%	%
RE	-45	90.72	76.66	62.12	14.06	28.60	15.50	31.52	3.13	22.57	6.13	44.24
L75	45	96.18	77.15	70.03	19.03	26.15	19.78	27.19	2.38	21.61	3.92	35.56

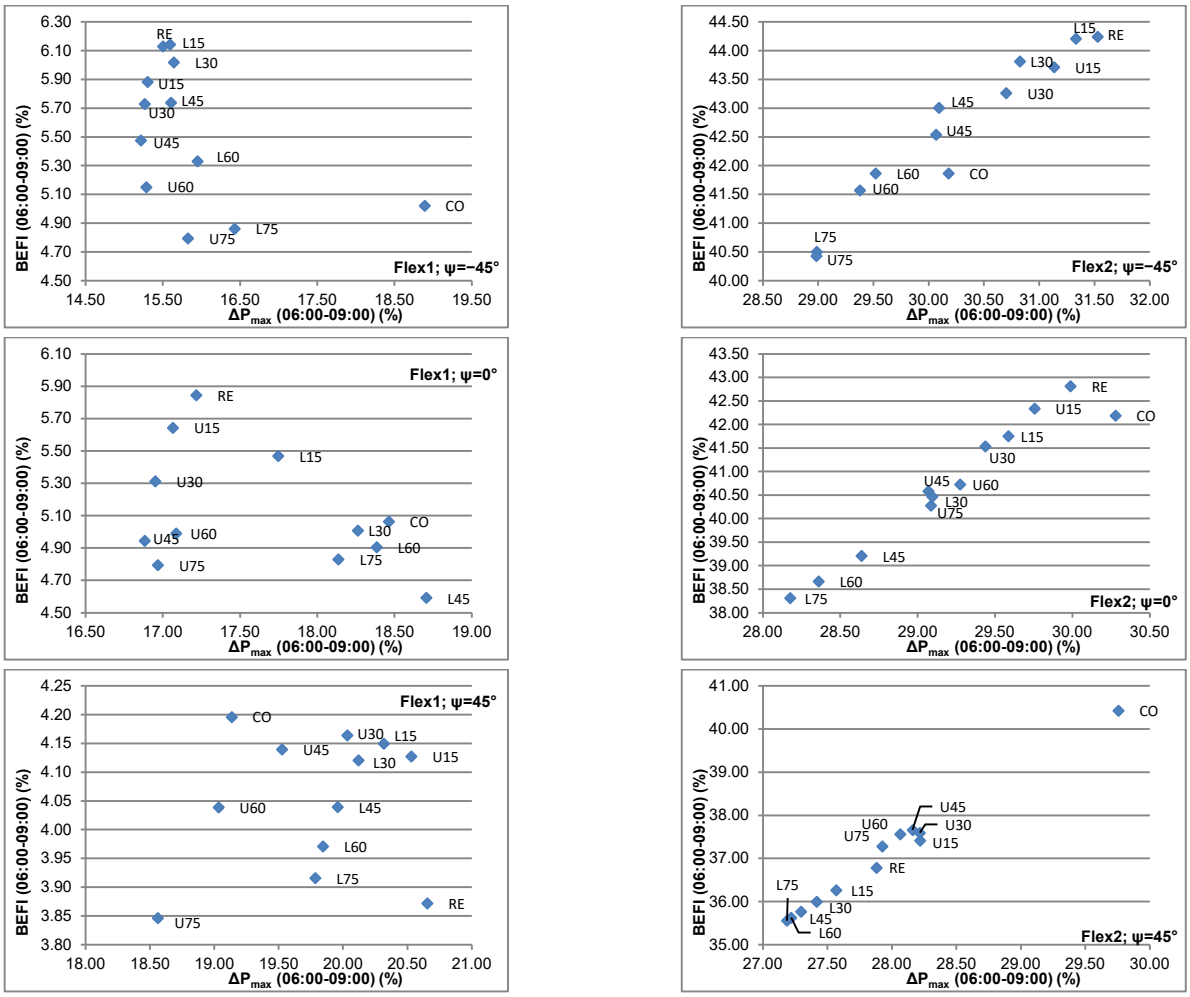

Figure 4: Comparison of Peak power reduction (%) and average BEFI (%) for the morning peak demand period (06:00 – 09:00); plan shape configurations at ψ=−45°, 0°, 45°; and Flex1, and Flex2 controls; for a cold sunny January day.

ΔP_{max} and BEFI

The flexibility performance of all the plan shapes using the two flexibility control strategies were compared by peak power reduction, ΔP_{max}, and BEFI. A scatter plot in Figure 4 shows the results for the morning peak demand period for a cold sunny January day. Three azimuths are shown: −45° and 45° to represent the extreme cases, and 0° to represent the typically-considered ideal case for solar building design. The range of peak power reduction and BEFI is shown in Table 2. The biggest ΔP_{max} and BEFI was achieved by RE at −45°.

The RE shape had the best performance at −45°, Flex2 followed closely by the L15 shape. Both benefitted from having lots of PV and window area oriented to the early morning sun to help reduce the peak at 08:15. The RE and CO shapes had the best performance at 0°, Flex2 since they still received a lot of early morning solar gains. But for −45°, Flex 1, and 0°, Flex1, a Pareto front was formed.

At 45° it was clear the CO shape had the best performance for Flex2, but it was on the Pareto front in Flex1. CO had the lowest peak power at 45° across all plan shapes at 95.73 kW, 75.91 kW, and 65.94 kW for the reference, Flex1, and Flex2 strategies, respectively. However, the *percentage reduction* was greater for the other plan shapes in Flex1 putting CO near the back of the pack for ΔP_{max}.

Table 2: Peak power reduction (ΔP_{max}), building energy flexibility index (BEFI). and Rate M and time of use (TOU) energy cost savings. All values in %.

Metric	Flex1				Flex2			
%	Smallest	Plan shape	Largest	Plan shape	Smallest	Plan shape	Largest	Plan shape
ΔP_{max}	15.21	U45(ψ=-45°)	20.65	RE(ψ=45°)	27.18	L75(ψ=45°)	31.53	RE(ψ=-45°)
BEFI	3.85	U75(ψ=45°)	6.14	L15(ψ=-45°)	35.56	L75(ψ=45°)	44.24	RE(ψ=-45°)
Rate M	12.82	L75(ψ=45°)	14.59	L15(ψ=-45°)	17.28	L75(ψ=45°)	25.03	L15(ψ=-45°)
TOU	3.05	L75(ψ=45°)	4.30	RE(ψ=0°)	10.49	L75(ψ=45°)	15.49	RE(ψ=0°)

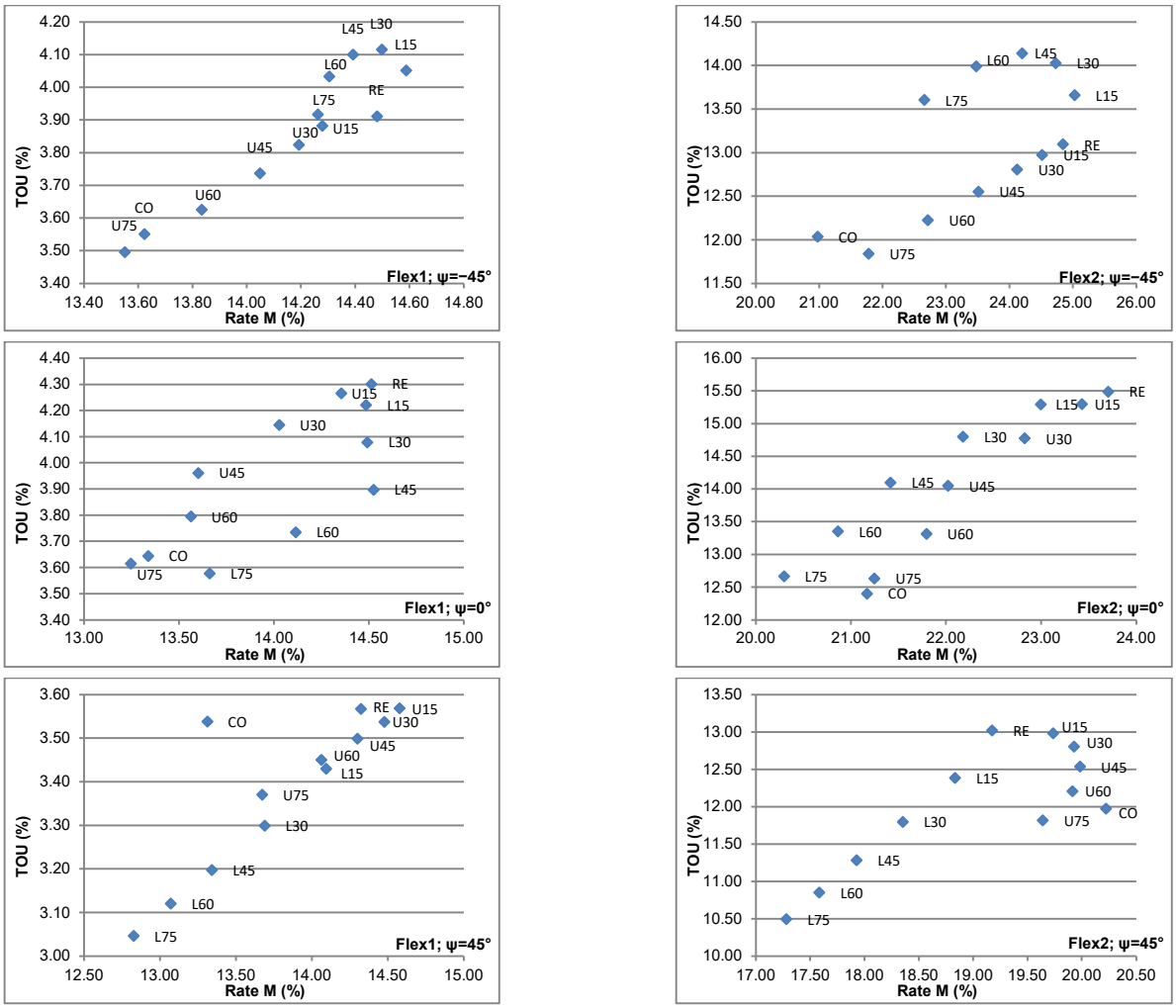

Figure 5: Comparison of energy cost savings (%) under Rate M and Time-of-use (TOU) pricing schemes; plan shape configurations at ψ=−45°, 0°, 45°; and Flex1, and Flex2 controls; for the month of January.

Overall, changing from Flex1 to Flex2 greatly increased the magnitude of the ΔP_{max} and BEFI and changed the configuration rankings for ΔP_{max} significantly.

Also, for Flex2, since peak power was reached during sunshine hours, the additional solar gains helped all configurations in the ΔP_{max} metric, including raising the performance of the L-shapes with small wing angles.

Rate M and TOU

The energy cost savings under the Rate M and TOU pricing schemes were compared for all plan shapes using the two flexibility control strategies. The results are shown at the same three azimuths as in the previous section for the month of January in the scatter plot in Figure 5.

The range of savings is shown in Table 2. Overall, the percentage energy cost savings were greater using Rate M than TOU (Table 2). The biggest savings using Rate M was achieved by L15 at −45°; and using TOU by RE at 0°.

At −45° the plan shapes with the most exposure to the morning sun had the most energy cost savings for both Rate M and TOU.

At 0° there was a clear best performer in RE in the Flex2 scenario. RE was also on the Pareto front in the Flex1 scenario. The plan shapes with large wing angles like L75 and U75 performed poorly due to diminished solar gains during midday and afternoon.

The configurations at ψ=45° were disadvantaged due to

Table 3: Rate M and time of use (TOU) energy cost savings for RE and CO plan shapes. All values in %.

Metric	Plan shape	Flex1			Flex2		
%		ψ=-45°	ψ=0°	ψ=45°	ψ=-45°	ψ=0°	ψ=45°
Rate M	RE	14.48	14.51	14.32	24.85	23.71	19.18
	CO	13.62	13.34	13.31	20.98	21.17	20.22
TOU	RE	3.91	4.30	3.57	13.10	15.49	13.02
	CO	3.55	3.65	3.57	12.04	12.40	11.97

this building type having its power peak in the morning. The ψ=45° orientation provided the least benefit for solar gains to help decrease the morning power peak. The L-shapes were particularly penalized due to this.

Changing from the Flex1 to the Flex2 strategy increased the energy cost savings for all configurations for Rate M and TOU, with the rankings generally unchanged. The exception was for the CO shape for Rate M.

The CO performance was the most consistent across azimuths for both Flex1 and Flex2, as shown in Table 3 in comparison to RE. The U75 shape had the second most consistent performance. It was the shape most similar to CO. The effect observed in Figure 5 was the other plan shapes' energy cost savings performance increasing and decreasing relative to CO. The consistency of the CO performance can be attributed to the fact that its plan shape is relatively orientation indifferent.

Across the two flexibility strategies, Rate M provided the most energy cost savings – significantly greater than TOU. This was due to the demand component of the pricing plan. While total energy may not change much, limiting power spikes greatly reduced the overall Rate M cost.

In the end, there was no scenario in which all metrics – ΔP_{max}, BEFI, Rate M, TOU – were in agreement on the best performing configuration. However, RE at ψ=0°, Flex2 control was close, being the best performing plan shape for Rate M and TOU energy savings and being one of two best plan shapes for ΔP_{max} and BEFI.

Conclusion

An automated design framework for BIPV/T NZEBs to support design decision-making at the early-design phase was used to investigate the influence of building form related variables on energy flexibility. The flexibility objective was to reduce peak power demand during the weekday 06:00 – 09:00 winter peak period in Quebec. Two energy flexibility controls based on rule-based setpoint controls were tested. The flexibility performance was measured by the peak power reduction, building energy flexibility index (BEFI), and energy cost savings based on two different energy pricing schemes – one with a peak demand charge, the other based on time-of-use rates.

The results showed that:

- The peak power could be reduced by 15% to 32%;
- The amount of flexible power made available to the grid using BEFI was 4% to 44% of reference power;
- Energy cost savings of 13% to 25% could be achieved under Rate M – which includes a demand charge;
- Energy cost savings of 3% to 15% could be achieved under a three-tiered time-of-use pricing scheme;
- The performance rankings under Flex1 and Flex2 generally agreed for energy cost savings but were significantly different for peak power reduction and BEFI; the magnitude of power reduction and energy cost savings was larger in Flex2;
- There was no scenario of azimuth/flexibility control in which all metrics agreed on the best performing plan shape. For most scenarios, performance comparisons over pairs of metrics resulted in a Pareto front of favourable plan shapes;
- The peak power reduction and BEFI metrics agreed on best performing plan at −45°, Flex2, being the rectangle; and at 45°, Flex2 being the courtyard shape;
- Rate M achieved much greater energy cost savings than TOU for the same orientation and flexibility control scenarios. Both found that at 0°, Flex2, the rectangle plan produced the most energy cost savings;
- The courtyard plan shape produced the most consistent energy cost savings across pricing scheme, orientation, and flexibility control; and the most consistent peak power reductions and BEFI flexible power across orientations for the Flex2 control.

The method and results provide early design stage support for building designers not normally involved in energy flexibility design. A wide range of orientations were studied to account for site design conditions or constraints. By making flexibility-aware design choices upstream of building controls, the building has potentially better flexibility performance once controls design begins.

Acknowledgments

This work was supported by the Natural Sciences and Engineering Research Council of Canada/Hydro-Québec Industrial Research Chair in Optimized Operation and Energy Efficiency: Towards High Performance Buildings; and the Fonds de recherche du Québec – Nature et technologies.

References

Aelenei, D., R. A. Lopes, L. Aelenei and H. Gonçalves (2019). "Investigating the potential for energy flexibility in an office building with a vertical BIPV and a PV roof system." Renewable Energy: 189-197.

Aguacil, S., S. Lufkin and E. Rey (2019). "Active surfaces selection method for building-integrated photovoltaics (BIPV) in renovation projects based on self-consumption and self-sufficiency." Energy and Buildings **193**: 15-28.

Athienitis, A. K., E. Dumont, J. A. Candanedo, N. Morovat, K. Lavigne and J. Date (2020). Development of a dynamic energy flexibility index for buildings and their interaction with smart grids. 2020 ACEEE summer study on energy efficiency in buildings, Virtual, ACEEE.

Barrutieta, X., A. Kolbasnikova, O. Irulegi and R. Hernández (2023). "Decision-making framework for positive energy building design through key performance indicators relating geometry, localization, energy and PV system integration." Energy and Buildings **297**.

Ciardiello, A., F. Rosso, J. Dell'Olmo, V. Ciancio, M. Ferrero and F. Salata (2020). "Multi-objective approach to the optimization of shape and envelope in building energy design." Applied Energy **280**: 115984.

D'Agostino, D., S. Mazzella, F. Minelli and F. Minichiello (2022). "Obtaining the NZEB target by using photovoltaic systems on the roof for multi-storey buildings." Energy and Buildings **267**.

Date, J., J. A. Candanedo and A. K. Athienitis (2021). "A methodology for the enhancement of the energy flexibility and contingency response of a building through predictive control of passive and active storage." Energies **14**(5).

Dumoulin, R., E. D. Rounis and A. Athienitis (2021). "Operation and grid interaction modeling of a house with a building integrated photovoltaic thermal (BIPV/T) system coupled to an air-source heat pump." Science and Technology for the Built Environment **27**(9): 1311-1329.

Freitas, S., C. Reinhart and M. C. Brito (2018). "Minimizing storage needs for large scale photovoltaics in the urban environment." Solar Energy **159**: 375-389.

Gaucher-Loksts, E., A. Athienitis and M. Ouf (2022). "Design and energy flexibility analysis for building integrated photovoltaics-heat pump combinations in a house." Renewable Energy **195**: 872-884.

Hydro-Québec (2023). 2023 Electricity Rates. Montreal, QC, Hydro-Québec.

Hydro-Québec. (2024). "Using energy more wisely in cold weather." Retrieved 01 March 2024, 2024, from http://www.hydroquebec.com/residential/customer-space/electricity-use/winter-electricity-consumption.html.

Jensen, S. Ø., A. Marszal-Pomianowska, R. Lollini, W. Pasut, A. Knotzer, P. Engelmann, A. Stafford and G. Reynders (2017). "IEA EBC Annex 67 Energy Flexible Buildings." Energy and Buildings **155**: 25-34.

Kurdi, Y., B. J. Alkhatatbeh and S. Asadi (2022). "The role of demand energy profile on the optimum layout of photovoltaic system in commercial buildings." Energy and Buildings **271**.

Le Dréau, J. and P. Heiselberg (2016). "Energy flexibility of residential buildings using short term heat storage in the thermal mass." Energy **111**: 991-1002.

Li, H. and T. Hong (2023). "On data-driven energy flexibility quantification: A framework and case study." Energy and Buildings **296**.

Li, H., H. Johra, F. de Andrade Pereira, T. Hong, J. Le Dréau, A. Maturo, M. Wei, Y. Liu, A. Saberi-Derakhtenjani, Z. Nagy, A. Marszal-Pomianowska, D. Finn, S. Miyata, K. Kaspar, K. Nweye, Z. O'Neill, F. Pallonetto and B. Dong (2023). "Data-driven key performance indicators and datasets for building energy flexibility: A review and perspectives." Applied Energy **343**.

Li, H., Z. Wang, T. Hong and M. A. Piette (2021). "Energy flexibility of residential buildings: A systematic review of characterization and quantification methods and applications." Advances in Applied Energy **3**.

Li, R., A. J. Satchwell, D. Finn, T. H. Christensen, M. Kummert, J. Le Dréau, R. A. Lopes, H. Madsen, J. Salom, G. Henze and K. Wittchen (2022). "Ten questions concerning energy flexibility in buildings." Building and Environment **223**: 109461.

Lind, J., E. Möllerström, H. Averfalk and F. Ottermo (2023). "Energy flexibility using the thermal mass of residential buildings." Energy and Buildings **301**.

Lovati, M., G. Salvalai, G. Fratus, L. Maturi, R. Albatici and D. Moser (2019). "New method for the early design of BIPV with electric storage: A case study in northern Italy." Sustainable Cities and Society **48**.

Martín-Chivelet, N. and D. Montero-Gómez (2017). "Optimizing photovoltaic self-consumption in office buildings." Energy and Buildings **150**: 71-80.

Morovat, N., A. K. Athienitis and J. A. Candanedo (2021). Application of Grey-Box Models for the Quantification of the Energy Flexibility of a School Building in Canada. ASHRAE Transactions.

Ontario Energy Board (2024). Historical electricity rates. Toronto, Ontario Energy Board.

Skandalos, N. and D. Karamanis (2021). "An optimization approach to photovoltaic building integration towards low energy buildings in different climate zones." Applied Energy **295**.

Tumminia, G., F. Guarino, S. Longo, D. Aloisio, S. Cellura, F. Sergi, G. Brunaccini, V. Antonucci and M. Ferraro (2020). "Grid interaction and environmental impact of a net zero energy building." Energy Conversion and Management **203**.

Yip, S., A. Athienitis and B. Lee (2021). Influence of early stage design variables and thermal mass on energy flexibility in net-zero energy buildings. eSIM 2021. IBPSA Canada. Vancouver, BC, IBPSA Canada.

Yip, S., A. K. Athienitis and B. Lee (2021). "Early stage design for an institutional net zero energy archetype building. Part 1: Methodology, form and sensitivity analysis." Solar Energy **224**: 516-530.

Zhang, K. and M. Kummert (2021). "Evaluating the impact of thermostat control strategies on the energy flexibility of residential buildings for space heating." Building Simulation **14**(5): 1439-1452.